IUST
Iran University of Science and Technology

Iranian Journal of Electrical and Electronic Engineering

Journal Homepage: ijeee.iust.ac.ir

A New DPC-SVM for Matrix Converter Used in Wind Energy Conversion System Based on Multiphase Permanent Magnet Synchronous Generator

E. Bounadja*(C.A.), Z. Boudjema* and A. Djahbar*

Abstract: This paper proposes a novel wind energy conversion system based on a Five-phase Permanent Magnetic Synchronous Generator (5-PMSG) and a Five to three Matrix Converter (5-3MC). The low cost and volume and also eliminating grid side converter controller are attractive aspects of the proposed topology compared to the conventional with back-to-back converters. The control of active and reactive power injected to the grid from the proposed system is carried out by a Direct Power Control (DPC) combined with a Space Vector Modulation (SVM). An advantage of this control, compared with the Conventional Direct Power Control (C-DPC) method, is that it eliminates the lookup table and lowers grid powers and currents harmonics through the use of a standard PI controller instead of hysteresis comparators. The efficiency of proposed whole system has been simulated by using MATLAB/Simulink environment.

Keywords: Five-Phase Permanent Magnetic Synchronous Generator (5-PMSG), Five to Three-Phase Matrix Converter (5-3MC), Grid Active and Reactive Powers, Direct Power Control (DPC), Space Vector Modulation (SVM), Wind Turbine.

1 Introduction

NOWADAYS the wind turbine conversion systems using the direct-driven three-phase Permanent Magnet Synchronous Generator (PMSG) are suitable and promising for application in wind farms [1-4]. The PMSG can be constructed with a large number of poles and can be operated as low speed direct-driven system without gearbox. This results in reduction of installation and maintenance costs and provides an advantage over the other types of generators. Furthermore, it has many advantages over induction generator, including: higher reliability, higher power, higher efficiency, higher torque, and simple control methods [3, 4]. On the other hand, multiphase PMSG shows other advantages over PMSG, such as reducing the amplitude and increasing the frequency of torque pulsations and higher reliability [5-7]. Therefore, multiphase PMSG is very attractive for application of renewable energy [8].

Several works on five phase PMSG based wind turbine with back-to-back converters have been studied recently as in [5-7]. However, the cost, volume and the number of power electronic converters increase the complexity of this topology. Due to these disadvantages, the MC can be used as an alternative to DC-link voltage-sourced converter for wind energy conversion systems. In addition, the main advantages of the MC are the ability to generate sinusoidal input-output voltage and current and the possibility of adjusting input power factor [8-14]. On the other hand, MC application has been adapted for specific objectives and has not been generalized for wind power conversion systems based on multiphase PMSG generators as in [10-14, 17, 18].

A review of the existing literature, the author in [8] proposed a wind energy conversion systems based on MC. The system studied by this author is based on a six-phase asymmetrical squirrel cage induction generator (SCIG) and MC as power electronic interface between six-phase SCIG and electrical network. However, the power control injected to the grid from this system has

Iranian Journal of Electrical and Electronic Engineering, 2019.
Paper first received 26 July 2018 and accepted 18 February 2019.
* The authors are with the Department of Electrical Engineering, University of Hassiba Benbouali, Chlef, Algeria.
E-mails: e.bounadja@univ-chlef.dz, Z.Boudjema@univ-chlef.dz and a.djahbar@univ-chlef.dz.
Corresponding Author: E. Bounadja.

not been investigated. In this purpose, our article focuses on this issue and investigates the control of 5-phase PMSG in wind energy conversion system based on MC.

Most of studies for the control of PMSG based wind turbine have focused recently. For example, [3] proposed an improvement vector control algorithms for the machine side converter and for the grid side converter. The control of active and reactive power has been applied with the application of voltage oriented control. However, this strategy requires rotary coordinate transformation and depends on the system parameters.

One of most and recent methods in controlling wind powers is the Conventional Direct Power Control (C-DPC). This method is characterized by its fast dynamic response, simple structure and robust response against parameter variation. In C-DPC strategy, active and reactive powers are estimated, using current measurements, controlled directly with hysteresis comparators and using a switching table similar to the one used in direct torque control (DTC) applied for AC machines as presented in [15,16].

The use of the DPC method in wind energy conversion systems based on PMSG has been the subject of a few studies. Study [4] proposed a PMSG connected to the grid via back to back converter. In this paper, the control of machine side converter is achieved by a conventional DTC and the grid side converter is controlled by a DPC. However, the most significant drawback of the this strategy is the variable switching frequency which mainly depends on the sampling frequency, the switching table structure, hysteresis bands, and the converter switching status. This variable switching frequency will produce a broadband harmonic spectrum in the AC line currents. For this reason, the design of filters in the AC line will be difficult and expensive [17, 19]. To surmount this inconvenience, we replace hysteresis comparators and swishing table existing in C-DPC by PI regulators with SVM resulting in a constant switching frequency of the power converter.

There are no researches in literature, to the best of our knowledge, of the use of DPC-SVM for the 5-phase PMSG based wind turbine using a 5-3MC. In this context, the present study was an attempt to combine the DPC approach with SVM for 5-phase PMSG connected to the grid via 5-3MC. This combination enables 5-phase PMSG based wind turbine to obtain the unit input power factor and lowers the grid powers and current harmonics. Therefore, it improves the control performance of the system. In addition, the propounded approach eliminates the lookup table and the nonlinearity effect of the hysteresis blocks through the use of the PI controller. Finally, a comparison of whole system performances, obtained by the proposed DTC-SVM and those determined by the C-DPC, is presented and validated by simulation in Matlab/Simulink.

2 General System Description

As shown in Fig.1, the system analysed is a variable speed wind turbine based on a 5-PMSG and 5-3MC connected to the grid via RL filter. Due to the low generator speed, the rotor shaft is coupled directly to the generator, which means that no gearbox is needed.

2.1 Wind Turbine Aerodynamic Model

The mechanical power produced by wind turbine can be expressed as below:

$$P_m = \frac{1}{2}\rho A C_P(\lambda,\beta)\, v_w^3 \tag{1}$$

where: ρ is air density, $A = \pi R^2$ is area swept by the rotor blades, R is turbine blade radius, C_p is wind turbine power coefficient, β is blade pitch angle, v_w is wind speed, λ is tip speed ratio, which is defined as:

$$\lambda = \frac{\Omega_m R}{v_w} \tag{2}$$

where Ω_m is angular speed of turbine rotor.

The mechanical equation of wind turbine system is given by:

$$T_m + T_{em} = K_f \Omega_m + J\frac{d\Omega_m}{dt} \tag{3}$$

where T_m is the mechanical torque of wind turbine, T_{em} is the electromagnetic torque of generator, J is the total inertia of the system, K_f is the coefficient of viscous friction.

The power coefficient C_p can be approximated, as relationship of tip speed ratio λ and blade pitch angle β, by the following expression [4]:

$$C_p(\lambda,\beta) = C_1\left(C_2\left(\frac{1}{\lambda+0.08\beta}-\frac{0.035}{\beta^3+1}\right)-C_3\beta-C_4\right)\times \exp\left(-C_5\left(\frac{1}{\lambda+0.08\beta}-\frac{0.035}{\beta^3+1}\right)\right)+C_6\lambda \tag{4}$$

where C_1 = 0.5176, C_2 = 116, C_3 = 0.4, C_4 = 5, C_5 = 21, C_6 = 0.0068.

2.2 Modelling of 5-PMSG

The stator voltage equations of the 5-PMSG in the

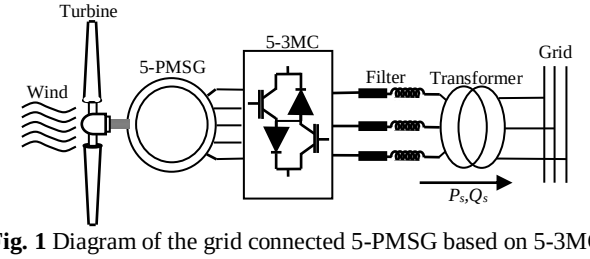

Fig. 1 Diagram of the grid connected 5-PMSG based on 5-3MC.

synchronous rotating *dq* reference frame can be described as follows [5-7]:

$$\begin{cases} v_d = Ri_d + \dfrac{d\psi_d}{dt} - \omega_m \psi_q \\ v_q = Ri_q + \dfrac{d\psi_q}{dt} + \omega_m \psi_d \end{cases} \quad (5)$$

The components of stator flux vector in this reference frame can be given by:

$$\begin{cases} \psi_d = Li_d \\ \psi_q = Li_q + \psi_f \end{cases} \quad (6)$$

The additional stator equations, which describe the generator in the (x–y) plane, are:

$$\begin{cases} v_x = Ri_x + \dfrac{d\psi_x}{dt} \\ v_y = Ri_y + \dfrac{d\psi_y}{dt} \end{cases} \quad (7)$$

$$\begin{cases} \psi_x = Li_x \\ \psi_y = Li_y \end{cases} \quad (8)$$

The electromagnetic torque of 5-PMSG can be expressed by the following equation:

$$T_{em} = \frac{5}{2} p \psi_f i_q \quad (9)$$

2.3 Five to three-phase MC

The topology of the 5-3MC discussed in this paper is shown in Fig. 2. Its configuration is fictitiously divided into a rectifier input stage and an inverter output stage, which are directly connected on the DC side. In inverter output stage, SVM method is applied for output voltage space vectors. Then the AC-AC converter is derived by eliminating the fictitious DC link.

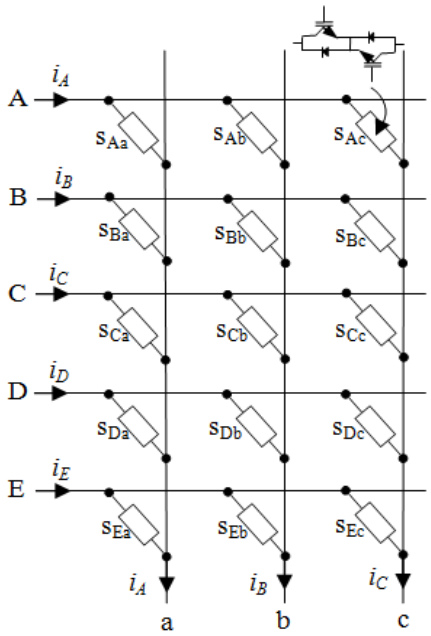

Fig. 2 The simplified topology of 5-3MC.

The switching function of each electronic power switch of the considering 5-3MC is defined as follows:

$$S_{mn} = \begin{cases} 1 \text{ if } S_{mn} \text{ closed} & m \in \{A,B,C,D,E\}, \\ 0 \text{ if } S_{mn} \text{ open} & n \in \{a,b,c\} \end{cases} \quad (10)$$

The input phase should never be short-circuited; therefore, only one switch can be in on-state in each leg at any instant:

$$S_{An} + S_{Bn} + S_{Cn} + S_{Dn} + S_{En} = 1, \quad n \in \{a,b,c\} \quad (11)$$

The proposed 5-3MC output phase voltages are made up of from its input phase voltages as below:

$$\begin{bmatrix} V_a \\ V_b \\ V_c \end{bmatrix} = \begin{bmatrix} S_{Aa} & S_{Ba} & S_{Ca} & S_{Da} & S_{Ea} \\ S_{Ab} & S_{Bb} & S_{Cb} & S_{Db} & S_{Eb} \\ S_{Ac} & S_{Bc} & S_{Cc} & S_{Dc} & S_{Ec} \end{bmatrix} \begin{bmatrix} V_A \\ V_B \\ V_C \\ V_D \\ V_E \end{bmatrix} \quad (12)$$

2.3.1 Five-Phase Rectifier Input Stage

According to Fig.3, the virtual intermediate voltage V_{dc} can be deduced as below:

$$V_{dc} = V^+ - V^- \quad (13)$$

The virtual potentials V^+ and V^- will be varying as function of the five-phase inputs and the rectification control functions as follows:

$$\begin{bmatrix} V^+ \\ V^- \end{bmatrix} = \begin{bmatrix} A^+ & B^+ & C^+ & D^+ & D^+ \\ A^- & B^- & C^- & D^- & E^- \end{bmatrix} \begin{bmatrix} V_A \\ V_B \\ V_C \\ V_D \\ V_E \end{bmatrix} \quad (14)$$

where m^+ and m^- (m= {A, B, C, D, E}) are the rectification control functions, defined by:

$$m^+ = \begin{cases} 1 & \text{if } V_m \text{ is the most postive input phase} \\ 0 & \text{if not} \end{cases}$$

$$m^- = \begin{cases} 1 & \text{if } V_m \text{ is the most negative input phase} \\ 0 & \text{if not} \end{cases} \quad (15)$$

The virtual intermediate voltage V_{dc} are illustrated in Fig. 4.

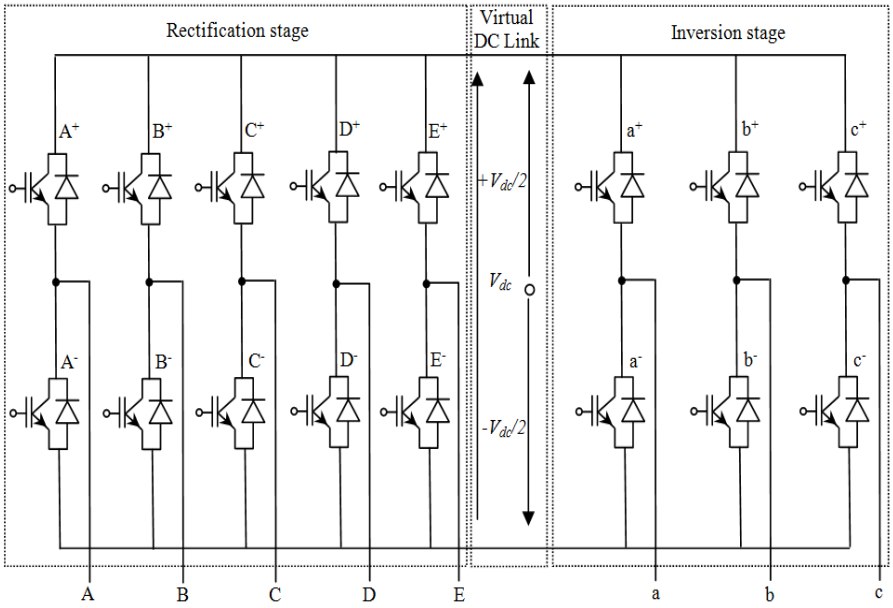

Fig. 3 The equivalent topology of 5-3MC.

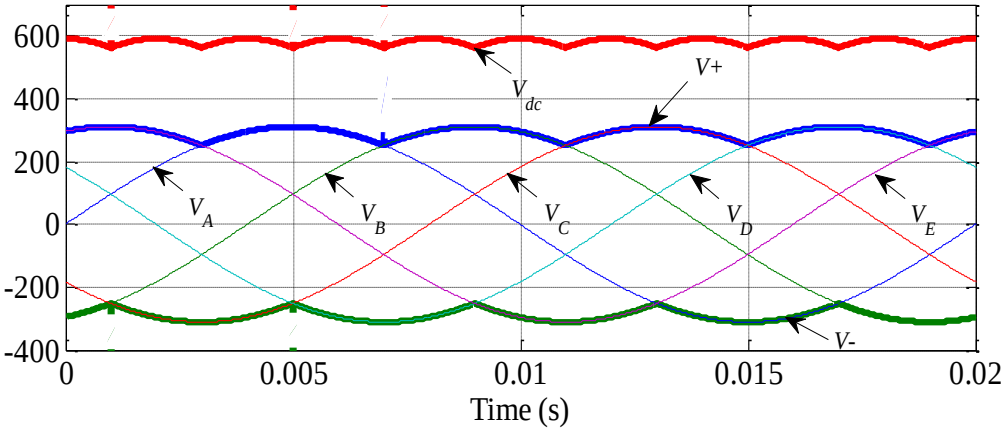

Fig. 4 Input voltages and virtual potentials.

2.3.2 Three-Phase Inverter Output Stage

A *Inverter* Output *Voltages*

The link between the virtual middle potential and the output voltages of 5-3MC (Fig. 3) is given as follows:

$$\begin{bmatrix} V_{ao} \\ V_{bo} \\ V_{co} \end{bmatrix} = \begin{bmatrix} a^+ & a^- \\ b^+ & b^- \\ c^+ & c^- \end{bmatrix} \begin{bmatrix} V^+ \\ V^- \end{bmatrix} \tag{16}$$

where n^+ and n^- (n= {a, b, c}) are the modulation functions (binary signals) similar to that used in conventional SVM control of standard inverter. It will be synthesizes in the following section.

B *SVM of Three-Phase Inverter Output Stage*

Six power switches have eight possible switching combinations in the Three-phase DC-AC converter. So there are 8 voltage space vectors defined by these 8 switching combinations, which consist of a circle including six effective space vectors and two zero ones. The circle is divided into 6 equal sectors. The demanded output voltage space vector V_s located in a sector can be synthesized by the adjacent two effective vectors and one zero vector consisting of this sector according to SVM method [19]. The basic output voltage space vectors and the corresponding switching states are represented in Fig. 5.

Suppose V_s locates in the sector k which is made up of two adjacent effective vectors V_k , V_{k+1} and a zero one V_z (Z=0, 7), and V_s leads α-axis by ϕ , then V_s can be composed of V_k , V_{k+1} and V_z , as below:

$$V_s = \frac{T_k}{T_s} V_k + \frac{T_{k+1}}{T_s} V_{k+1} + \frac{T_0}{T_s} V_z \tag{17}$$

with

$$T_k = \frac{\sqrt{3} T_s V_s}{V_{dc}} \sin(-\varphi + \frac{k\pi}{3}),\ T_{k+1} = \frac{\sqrt{3} T_s V_s}{V_{dc}} \sin(\varphi - \frac{(k-1)\pi}{3}),$$
$$T_0 = T_s - T_k - T_{k+1} \tag{18}$$

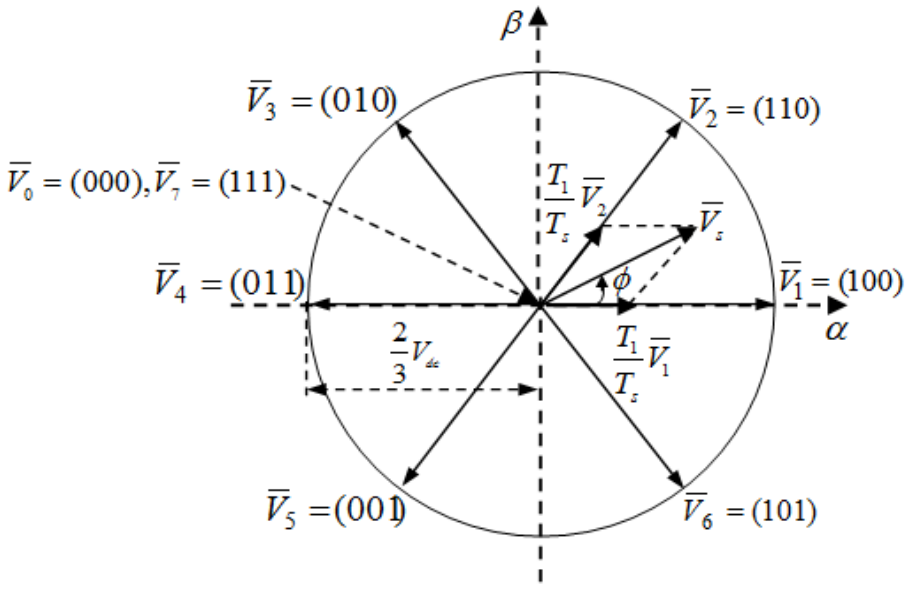

Fig. 5 Input voltages and virtual potentials.

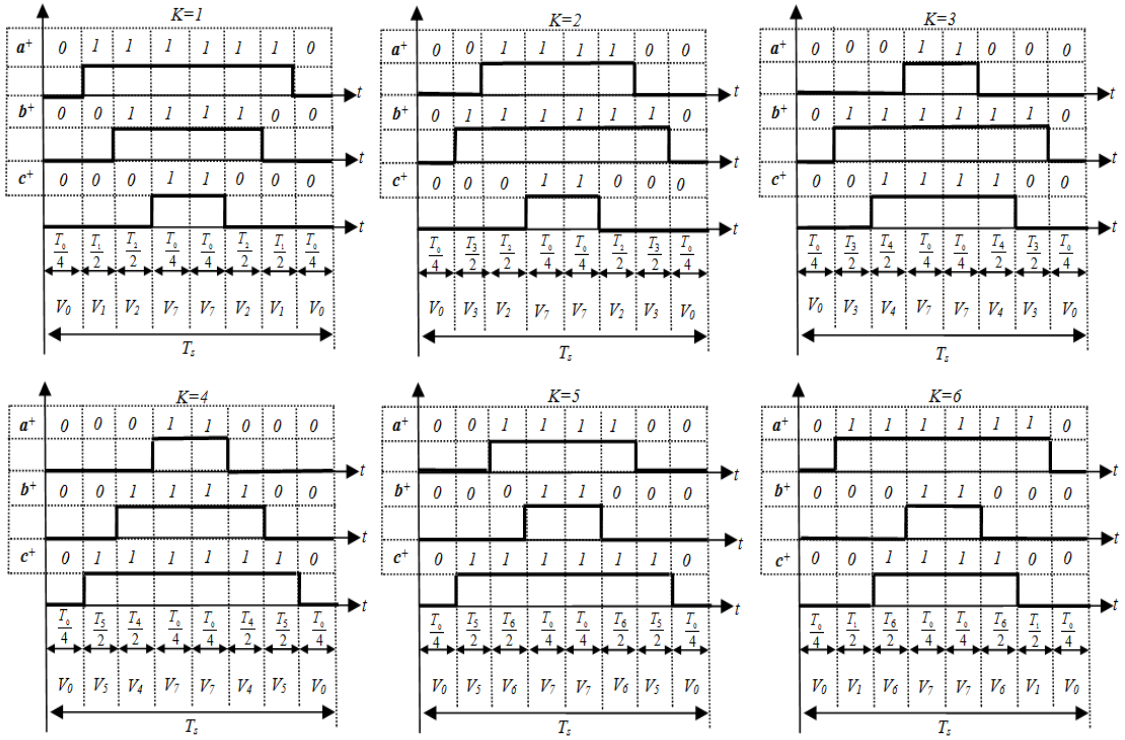

Fig. 6 Input voltages and virtual potentials.

where T_s is the switching period and T_k, T_{k+1}, T_0 are the switching-on time of voltage vectors V_k, V_{k+1} and V_z respectively.

The modulation functions n^+ (n= {a, b, c}) are obtained as represented in Fig. 6.

The modulation functions n^- (n= {a, b, c}) can similarly be obtained as fellow:

$$n^- = 1 - n^+ \tag{19}$$

2.3.3 Five to Three MC Switching Functions

The above-mentioned DC-link is imaginary that is say the rectifying and inverting of 5-3MC are conducted at the same time. Therefore this DC-link should be eliminated by substitution of (14) in (16), so, the output-line voltages are obtained as follows:

$$\begin{bmatrix} V_{ao} \\ V_{bo} \\ V_{co} \end{bmatrix} = \begin{bmatrix} a^+ & a^- \\ b^+ & b^- \\ c^+ & c^- \end{bmatrix} \begin{bmatrix} A^+ & B^+ & C^+ & D^+ & D^+ \\ A^- & B^- & C^- & D^- & E^- \end{bmatrix} \begin{bmatrix} V_A \\ V_B \\ V_C \\ V_D \\ V_E \end{bmatrix} \tag{20}$$

Equation (20) can be written as follow:

$$\begin{bmatrix} V_{ao} \\ V_{bo} \\ V_{co} \end{bmatrix} = \begin{bmatrix} \tau_{Aa} & \tau_{Ba} & \tau_{CA} & \tau_{Da} & \tau_{Ea} \\ \tau_{Ab} & \tau_{Bb} & \tau_{Cb} & \tau_{Db} & \tau_{Eb} \\ \tau_{Ac} & \tau_{Bc} & \tau_{Cc} & \tau_{Dc} & \tau_{Ec} \end{bmatrix} \begin{bmatrix} V_A \\ V_B \\ V_C \\ V_D \\ V_E \end{bmatrix} \tag{21}$$

where τ_{mn} represent the reference signals defined as follows:

$$\tau_{mn} = m^{+}n^{+} + m^{-}n^{-}, \quad m \in \{A,B,C,D,D,E\}, \quad n \in \{a,b,c\} \tag{22}$$

Based on (21) and on the conventional mathematical model of an inverter, the 5-3MC output voltages are expressed as below:

$$\begin{bmatrix} V_a \\ V_b \\ V_c \end{bmatrix} = \frac{1}{3}\begin{bmatrix} 2 & -1 & -1 \\ -1 & 2 & -1 \\ -1 & -1 & 2 \end{bmatrix} \begin{bmatrix} \tau_{Aa} & \tau_{Ba} & \tau_{CA} & \tau_{Da} & \tau_{Ea} \\ \tau_{Ab} & \tau_{Bb} & \tau_{Cb} & \tau_{Db} & \tau_{Eb} \\ \tau_{Ac} & \tau_{Bc} & \tau_{Cc} & \tau_{Dc} & \tau_{Ec} \end{bmatrix} \begin{bmatrix} V_A \\ V_B \\ V_C \\ V_D \\ V_E \end{bmatrix} \tag{23}$$

The similarly between (12) and (23), can deduce the 5-3MC switching functions as follows:

$$\begin{cases} S_{ma} = \frac{1}{3}(2\tau_{ma} - \tau_{mb} - \tau_{mc}) \\ S_{mb} = \frac{1}{3}(2\tau_{mb} - \tau_{ma} - \tau_{mc}), \quad m \in \{A,B,C,D,E\} \\ S_{mc} = \frac{1}{3}(2\tau_{mc} - \tau_{ma} - \tau_{mb}) \end{cases} \tag{24}$$

3 DPC-SVM of Grid Connected 5-PMSG

3.1 Control Scheme of DPC-SVM

The dynamic model of grid side electrical circuits is presented as [6]:

$$\begin{cases} v_{gd} = R_g i_{gd} + L_g \dfrac{di_{gd}}{dt} - \omega_g L_g i_{gq} + v_{cgd} \\ v_{gq} = R_g i_{gq} + L_g \dfrac{di_{gq}}{dt} - \omega_g L_g i_{gd} + v_{cgq} \end{cases} \tag{25}$$

where v_{gd} and v_{gq} are the dq components of the grid voltage vector, i_{gd} and i_{gq} are the dq components of the grid current vector; v_{gcd} and v_{gcq} are the dq components of the voltage vector of grid side converter, L_g and R_g are inductance and resistance of the grid filter, ω_g is angular frequency of the grid voltage.

In conventional DPC (C-DPC), the hysteresis controllers and switching table have been used. This control strategy is characterized by varied switching frequency of control signals. In the control system of 5-3MC considered in this paper, a DPC-SVM method has been applied. The block scheme of control system is presented in Fig. 7. This method has simple structure, low number of coordinates transformations and good dynamic properties. The temporary angle positions θ_g of the grid voltage vector are obtained from the Phase Locked Loop (PLL) block. The applied PLL system is a feedback system with PI-regulator tracking the phase angle of grid voltage vector [6].

The control algorithm of DPC-SVM is based on the active and reactive power estimator as [14]:

$$\begin{cases} p_g = \frac{3}{2}(V_{gd} i_{gd} + V_{gq} i_{gq}) \\ Q_g = \frac{3}{2}(V_{gq} i_{gd} - V_{gd} i_{gq}) \end{cases} \tag{26}$$

The control strategy of DPC-SVM for 5-3MC uses two control loops with PI controllers. These inner control loops regulate the active and reactive power of AC grid. The estimated values of active and reactive grid power are compared with the reference values. In the typical control systems, the reactive grid power reference is set to zero in order to perform the operation at unity power factor. The output signals from PI controllers determine the reference voltages $v_{gc\alpha\_ref}$ and $v_{gc\beta\_ref}$ for SVM of 5-3MC.

3.2 Synthesis of Grid Active and Reactive Power Controllers

To ensure a pure active power exchange from the wind generator and maintain the reactive power exchange to the grid, which guarantees a desirable power factor during the generator function, an orientation of d-axis of the synchronous reference frame with grid voltage vector is required [20, 21]. So (26) becomes as follows:

$$\begin{cases} v_{gd} = V_g \\ v_{gq} = 0 \end{cases} \tag{27}$$

The grid active and reactive power in (dq) coordinates has the form after orientation as below:

$$\begin{cases} p_g = \frac{3}{2} V_g i_{gq} \\ Q_g = \frac{3}{2} V_g i_{gd} \end{cases} \tag{28}$$

Based on the above equations, the schematic diagram of power control loops take the form as illustrated in Fig. 8.

4 Simulation Results

The simulation model of wind energy conversion

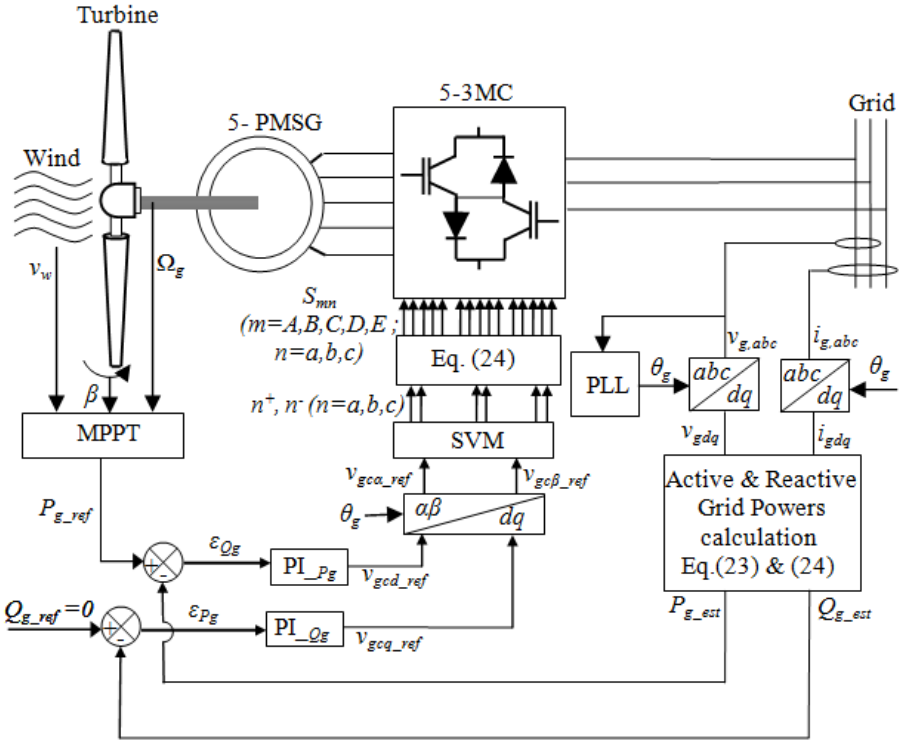

Fig. 7 Control diagram of DPC-SVM of the whole system.

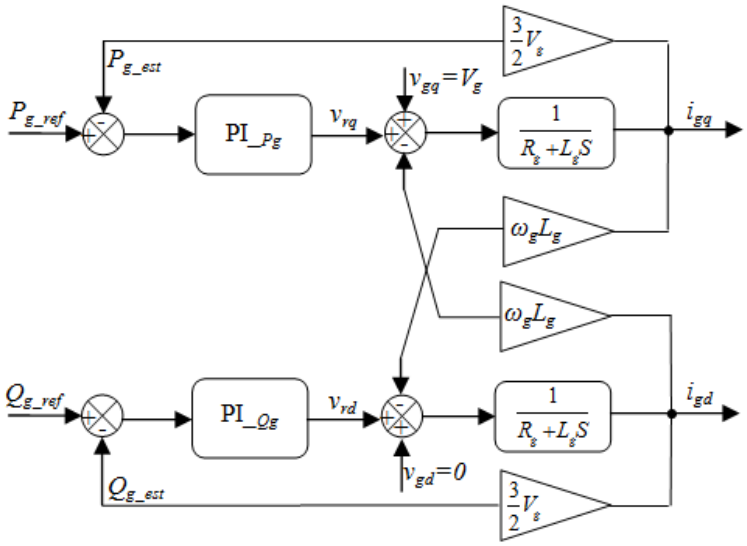

Fig. 8 Synthesis of grid active and reactive power controllers.

system with the considered control systems has been implemented in MATLAB/Simulink. The aim of simulation was the investigation of properties of control systems. The used wind turbine parameters are presented in Tables 1-3.

The obtained simulation results of considered wind energy conversion system are presented in Figs. 9-22.

The considered control of whole system has been tested for the wind speed v_w during the period of the 10s, while, the average wind speed v_{wa} has been adopted as equal to 11m/s as presented in Fig. 9.

Fig. 10 shows the waveforms of optimal $\Omega_{g\text{-}opt}$ and measured angular speed Ω_g of 5-PMSG obtained from simulation of control system. It can be seen, that the generator speed Ω_g is accurately adjusted to the waveforms of optimal speed $\Omega_{g\text{-}opt}$, which is obtained from MPPT algorithm.

The obtained waveforms of power coefficient C_p and tip speed ratio λ at various wind speeds have been presented in Figs. 11-12.

Fig. 13 presents the responses of electromagnetic torque T_{em} of 5-PMSG and mechanical torque T_m of

Table 1 Grid parameters.

Parameter	Value
Grid Frequency ω_g	2π50 [rad/s]
Grid resistance R_g	0.015 [Ω]
Grid inductance L_g	0.002 [H]

Table 2 Wind turbine parameters.

Parameter	Value
Rotor radius R	1.8 [m]
Air density ρ	1.225

Table 3 Five phase PMSG parameters.

Parameter	Value
Rated power P_n	4.8 [kW]
Rated Torque T_n	76 [N.m]
Pairs poles number p	5
Stator resistance R_s	0.425 [Ω]
Stator dq-axis inductance L_s	0.00835 [H]
Inertia J	0.01197 [kg.m^2]
Flux linkage ψ_f	0.433 [Wb]

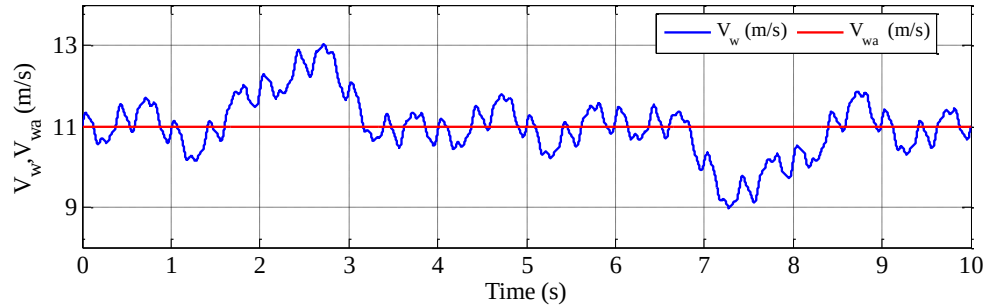

Fig. 9 Waveforms of average wind speed v_{wa} and real wind speed v_w [*m/s*].

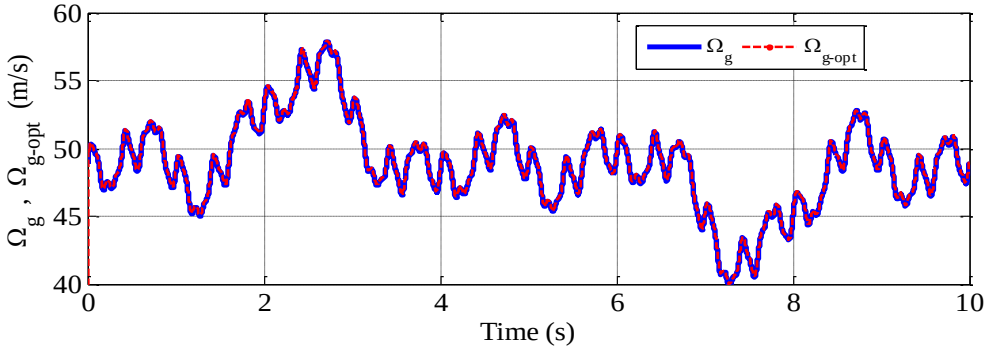

Fig. 10 Waveforms of the reference speed $\Omega_{g\text{-}opt}$ and the actual speed Ωg of PMSG.

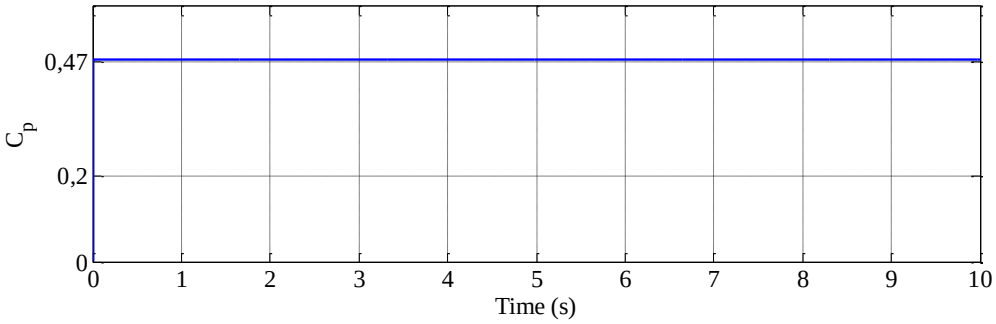

Fig. 11 Waveform of power coefficient of wind turbine C_p.

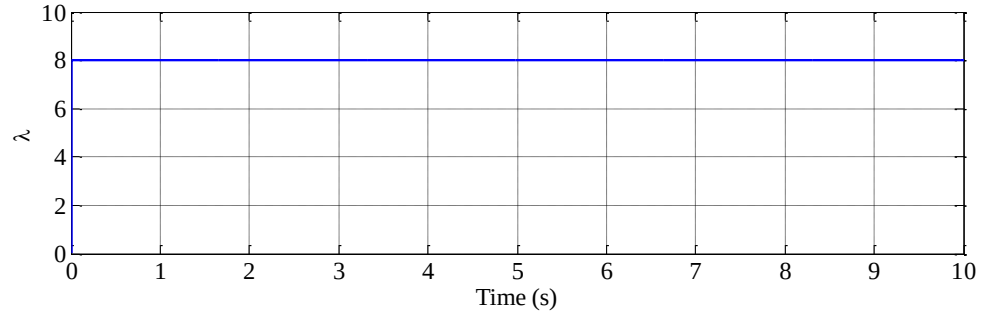

Fig. 12 Waveforms of tip speed ratio λ.

wind turbine during the considered variation of wind speed. The considered control system allows fast responses of the electromagnetic torque T_{em} of 5-PMSG during temporary time variations of the wind speed.

Figs. 14-15 show the waveforms of machine *dq*-axis and *xy*-axis currents. The response of current vector components (i_d, i_q) is practically changing according to variations of wind speed. However, the components (i_x, i_y) have been kept at zero value, as desired.

Figs. 16-17 display the three-phase current waveforms injected to the grid by the conversion system controlled by both C-DPC and DPC-SVM. It can be seen, that this current has a sinusoidal form and changing according to the variations of wind speed for both methods. The effectiveness of proposed strategy is shown in these figures. Also, Figs. 18-19 show the improvement of stator currents THD where it clear to see that by using the SVM strategy the current THD decreases justifying the use of the proposed control, (THD of 107.75 % for the C-DPC and 51.44% for the proposed DPC-SVM).

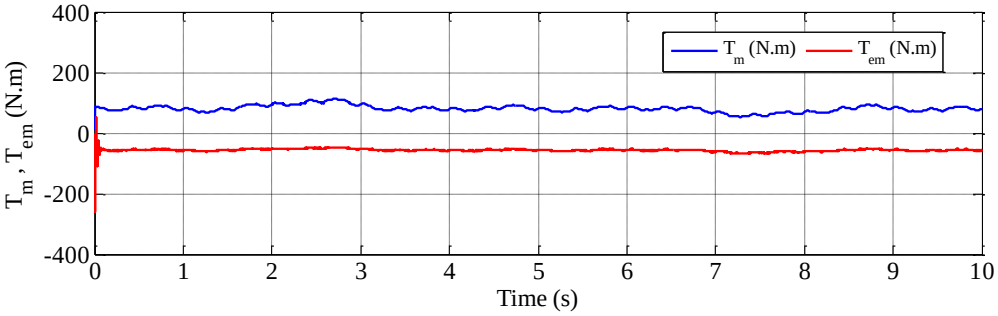

Fig. 13 Waveforms of electromagnetic torque T_{em} of 5-PMSG and mechanical torque T_m of wind turbine.

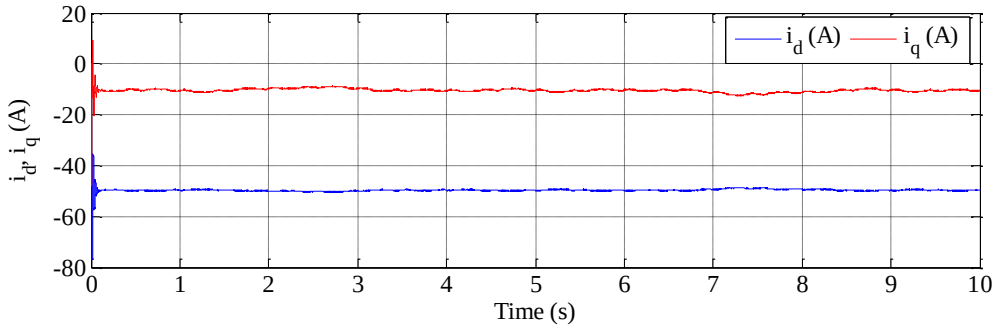

Fig. 14 5-PMSG *dq*-axis currents.

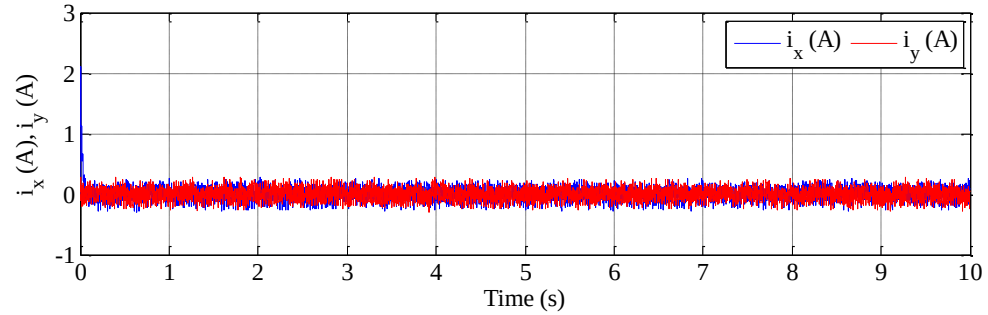

Fig. 15 5-PMSG *xy*-axis currents.

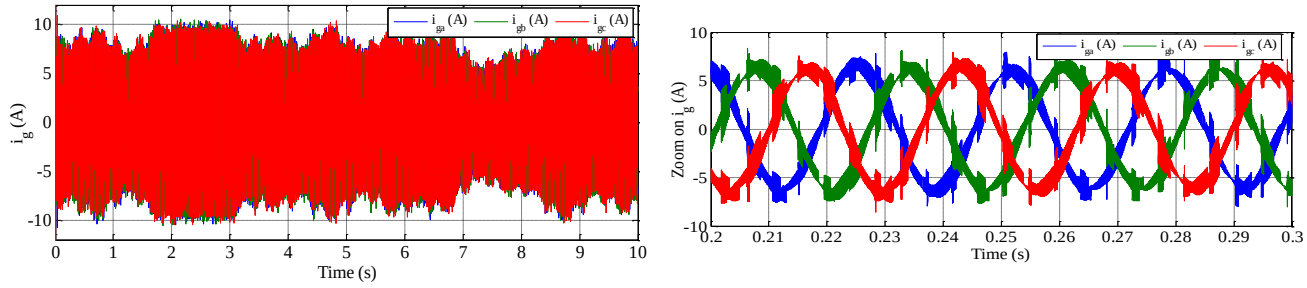

(a) (b)

Fig. 16 Three-phase grid current i_{ga}, i_{gb}, i_{gc} (A) (C-DPC).

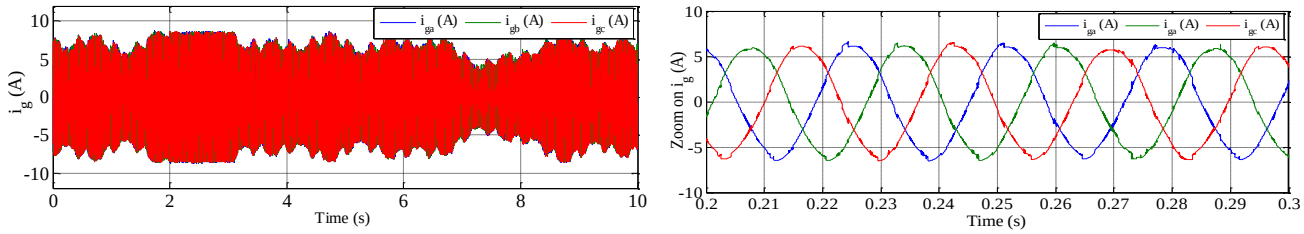

(a) (b)

Fig. 17 Three-phase grid current i_{ga}, i_{gb}, i_{gc} (A) (DPC-SVM).

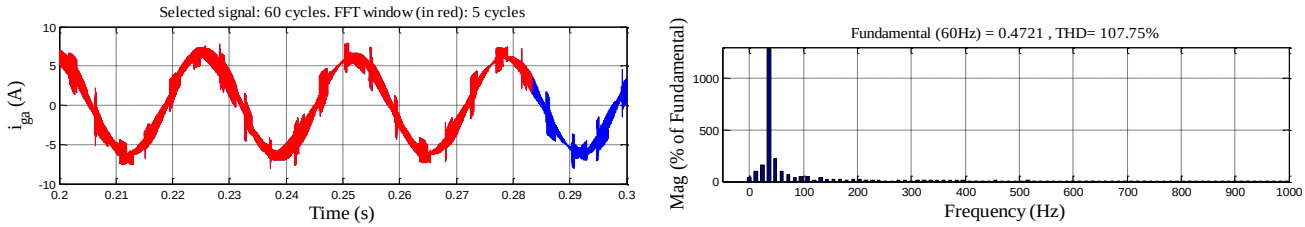

(a) (b)

Fig. 18 Phase a grid current THD (C-DPC).

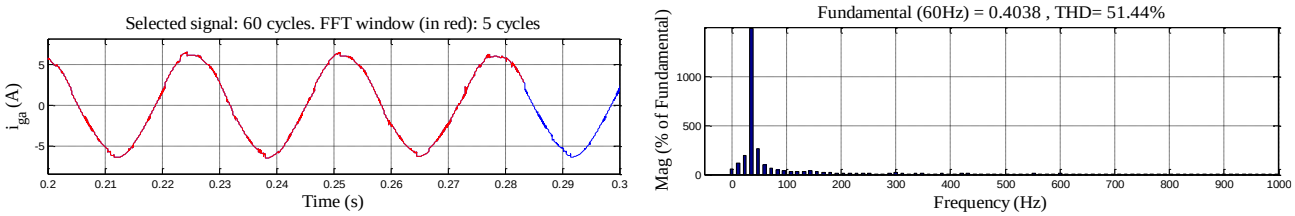

(a) (b)

Fig. 19 Phase a grid current THD (DPC-SVM).

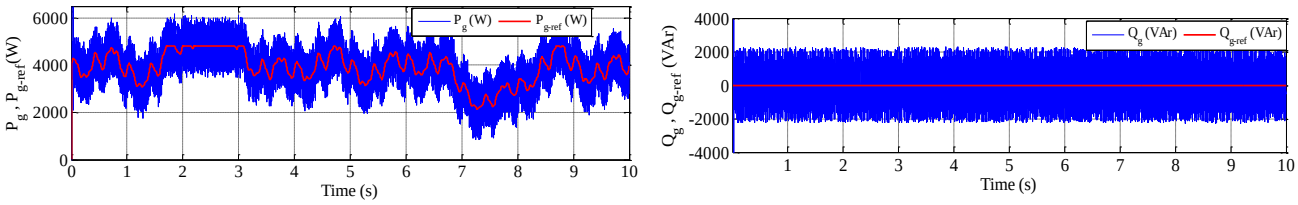

(a) (b)

Fig. 20 Waveforms of active and reactive grid power a) P_g and b) Q_g. (C-DPC).

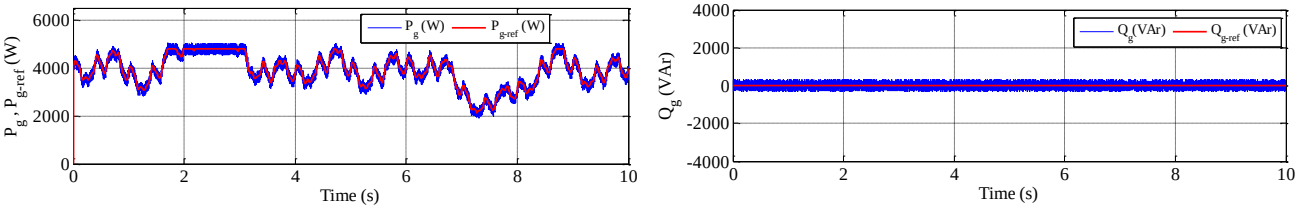

(a) (b)

Fig. 21 Waveforms of active and reactive grid power a) P_g and b) Q_g. (DPC-SVM).

In Fig. 20 the active and reactive powers injected to the grid, controlled via the proposed DPC-SVM, are displayed, while, in a comparative way, Fig. 21, describes these quantities under the conventional direct power control (C-DPC). One can conclude that, under the proposed control algorithm, the grid power amounts track their references values with smooth profiles, with ripple-free. Also, from these figures, it can be noticed, that only the active power generated by the proposed system is fully delivered to the AC grid, while the reactive power is equal to zero.

Finally, Fig. 22 shows the waveform of the grid voltage and current delivered by the generating system, between 0 s and 0.15 s. It can be seen that the voltage is in phase opposition with the current, which proves that the 5-PMSG, drives with unitary factor power, as can be checked on Fig. 21.

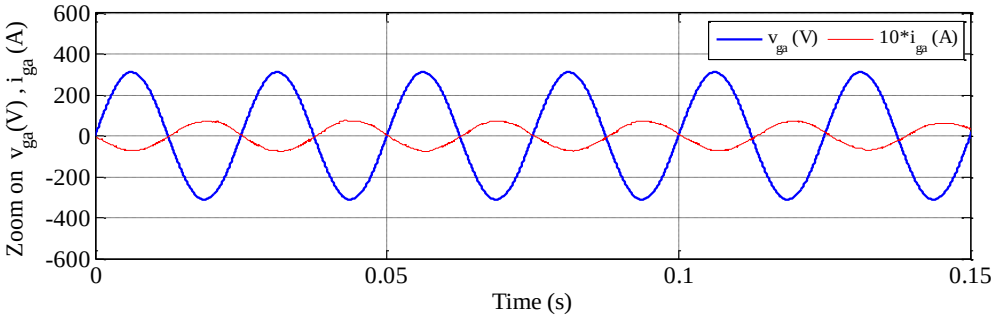

Fig. 22 Waveforms of grid phase voltage v_{ga} and current i_{ga} (DPC-SVM).

5 Conclusion

In this paper, a new scheme for grid connected 5-PMSG has been presented. The conventional back-to-back converter has been replaced by a 5-3MC. In the proposed scheme, bulky DC-link capacitors and also the grid side converter has been eliminated. In this study, a simple way to control the 5-3MC by considering a virtual DC link between two conversions stage (rectification and inversion) is used. In order to control the active and reactive power injected to the grid a DPC with SVM have been explored. This method eliminates the lookup table and reduces the grid powers and currents harmonics by replacing hysteresis comparators with PI controllers. Another advantage of the propounded approach is that it achieves the unit input power factor. A simulation of the considered control algorithms, with a suitable wind variation, has been applied to whole system. Simulation results show good performances. Therefore, the control method objectives are achieved.

References

[1] J. C. Hui, A. Bakhshai, and P. K. Jain, "An energy management scheme with power limit capability and an adaptive maximum power point tracking for small standalone PMSG wind energy systems," *IEEE Transactions on Power Electronics*, Vol. 31, No. 7, pp. 4861–4875, 2016.

[2] C. Wei, Z. Zhang, W. Qiao, and L. Qu, "An adaptive network-based reinforcement learning method for MPPT control of PMSG wind energy conversion systems," *IEEE Transactions on Power Electronics*, Vol. 31, No. 11, pp. 7837–7848, 2016.

[3] P. Gajewski and K. Pieńkowski, "Advanced control of direct-driven PMSG generator in wind turbine system," *Archives of Electrical Engineering*, Vol. 65, No.4, pp. 643–656, 2016.

[4] P. Gajewski and K. Pieńkowski, "Direct torque control and direct power control of wind turbine system with PMSG," *Przegląd Elektrotechniczny*, Vol. 92, No. 10, pp. 249–253, 2016.

[5] A. Youssef, A. Mahmoud, M. Sayed, N. Abdel-Wahab, and G. S. Salman, "MPPT control technique for direct-drive five-phase PMSG wind turbines with wind speed estimation," *International Journal of Sustainable and Green Energy*, Vol. 4, No. 5, pp. 195–205, 2015.

[6] S. Rhaili, A. Abbou, S. Marhraoui, and N. El Hichami, "Vector control of five-phase permanent magnet synchronous generator based variable-speed wind turbine," in *International Conference on Wireless Technologies, Embedded and Intelligent Systems (WITS)*, Fez, Morocco, 2017.

[7] H. H. Mousa, A. R. Youssef, and E. M. Mohamed, "Model predictive speed control of five-phase PMSG based variable speed wind generation system," in *Twentieth International Middle East Power Systems Conference (MEPCON)*, Cairo, Egypt, 2018.

[8] A. Djahbar, A. Zegaoui, and M. Aillerie, "Multiphase wind energy conversion systems based on matrix converter," *Automatika*, Vol. 57, No. 2, pp. 396–404, 2016.

[9] A. Badiee-Azandehi, A. Yousefi-Talouki, and M. Rezanejad, "Direct torque control space vector modulation of five-phase interior permanent magnet synchronous motor using matrix converter," *Australian Journal of Electrical & Electronics Engineering*, Vol. 12, No. 2, pp. 113–124, 2015.

[10] M. M. Rezaoui, L. Nezli, and M. O Mahmoudi, "High performances of five–phase induction machine feeding by a [3×5] Matrix Converter", *Journal of Electrical Engineering*, Vol. 65, No. 2, pp. 83–89, 2014.

[11] M. M. Rezaoui, L. Nezli, M. O. Mahmoudi, A. Kouzou, and H. Abu Rub, "A modified PWM three intervals control for a matrix converter in real time," *Archives of Control Sciences*, Vol. 3, No. 1, pp. 85–98, 2014.

[12] K. You, D. Xiao, M. F. Rahman, and M. N. Uddin, "Applying reduced general direct space vector modulation approach of AC-AC matrix converter theory to achieve direct power factor controlled three-phase AC-DC matrix rectifier," *IEEE Transactions on Industry Applications*, Vol. 50, pp. 2243–2257, 2014.

[13] H. Nikkhajoei, A. Tabesh, and R. Iravani, "Dynamic model of a matrix converter for controller design and system studies," *IEEE Transactions on Power Delivery*, Vol. 21, pp. 744–754, 2006.

[14] C. Klumpner, F. Blaabjerg, I. Boldea, and P. Nielsen, "New modulation method for matrix converters", *IEEE Transactions on Industry Applications*, Vol. 42, pp. 797–806, 2006.

[15] L. Xu and P. Cartwright, "Direct active and reactive power control of DFIG for wind energy generation," *IEEE Transactions on Energy Conversion*, Vol. 21, No. 3, pp. 750–758, 2006.

[16] R. Datta and V. T Ranganathan, "Direct power control of grid-connected wound rotor induction machine without rotor position sensors," *IEEE Transactions on Power Electronics*, Vol. 16, No.3, pp. 390–399, 2001.

[17] M. Jafari, K. Abbaszadeh, and M. Mohammadian, "A novel DTC-SVM approach for two parallel-connected induction motors fed by matrix converter," *Turkish Journal of Electrical Engineering & Computer Sciences*, Vol. 26, pp. 1599–1611, 2018.

[18] T. D. Nguyen and H. H. Lee, "Development of a three-to-five-phase indirect matrix converter with carrier-based PWM based on space-vector modulation analysis," *IEEE Transactions on Industrial Electronics*, Vol. 63, pp.13–24, 2016.

[19] T. Vajsz and L. Számel, "Improved modified DTC-SVM methods for increasing the overload-capability of permanent magnet synchronous motor servo- and robot drives–Part1," *Periodica Polytechnica Electrical Engineering and Computer Science*, Vol. 62, No. 3, pp. 65–73, 2018.

[20] B. K. O. Hasnaoui, M. Al Laqui, and J. Belhadj, "PMSG gear-less wind turbine equipped with an active and reactive power supervisory," *International Journal of Renewable Energy Research*, Vol. 4, No. 2, pp. 435–444, 2014.

[21] N. Freire, J. Estima, and A. Cardoso, "A comparative analysis of PMSG drives based on vector control and direct control techniques for wind turbine applications," *Przegląd Elektrotechniczny*, Vol. 88, No. 1, pp. 184–187, 2012.

E. Bounadja was born in Chlef, Algeria, in 1973. He received his Eng. and M.Sc. degrees in Electrical Engineering from the University of Hassiba Benbouali, Chlef, Algeria, in 1997 and 2008, respectively, and his Ph.D. degree in Electrical Engineering from the National Polytechnic School of Algiers, Algeria, in 2017. He is an Associate Professor at the Electrical Engineering Department of the University Hassiba Benbouali, Chlef, Algeria. His research activities include the power electronics, intelligent and robust controls in the wind-power systems.

Z. Boudjema was born in Chlef, Algeria, in 1983. He received his Eng. and M.Sc. degrees in Electrical Engineering from National Polytechnic School, Oran, Algeria, in 2006 and 2010, respectively, and his Ph.D. degree in Electrical Engineering from Djilali elyabes University, Sidi Belabès, Algeria, in 2015. He is an Associate Professor at the Electrical Engineering Department of the University Hassiba Benbouali, Chlef, Algeria. His research activities include application of robust control in the wind-solar power systems.

A. Djahbar was born in Chlef, Algeria, in February 1970. He received his Eng. and M.Sc. degrees in Electrical Engineering from the National Polytechnic School of Algiers, Algeria, in 1995 and 1998, respectively, and the Ph.D. degree in Electrical Engineering from the Mohamed Boudiaf University, Oran, Algeria, in 2008. He is a Full Professor at the Electrical Engineering Department of the University Hassiba Benbouali, Chlef, Algeria. His scientific work is related to multi machine drives, matrix converter and power quality.